KU-13-3

Skewed Steel Bridges, Part I: Effect of Cross-Frame Layout on Lateral Flange Bending Stresses

By

James Zhou

Caroline Bennett

Adolfo Matamoros

Jian Li

Stan Rolfe

A Report on Research Sponsored by
The Kansas Department of Transportation

Structural Engineering and Engineering Materials
SM Report No. 113
September 2015

THE UNIVERSITY OF KANSAS CENTER FOR RESEARCH, INC.

2385 Irving Hill Road – Campus West, Lawrence, Kansas 66045

Executive Summary

Lateral flange bending stresses can arise from a number of sources, such as wind loading or eccentric concrete placement, but of particular interest are lateral flange bending stresses, f_l, that occur due to skew. Lateral flange bending stresses that occur in skewed bridge systems tend to develop due to lateral forces transferred through cross-frames which may connect adjacent girders at different span points. In lieu of a refined analysis, the AASHTO-LRFD Bridge Design Specifications currently permit engineers examining bridges skewed more than 20° to use a minimum value of f_l = 10 ksi for an interior girder and f_l = 7.5 ksi for an exterior girder. The estimates for f_l provided within the AASHTO-LRFD Bridge Design Specifications are based on a limited data set for skewed bridges. Additionally, since the AASHTO-LRFD Design Specifications state that cross-frames or diaphragms should be placed in a staggered configuration when a bridge is skewed more than 20°, the approximate values provided for f_l should not be expected to be indicative of the lateral flange bending stresses experienced when cross-frames are instead carried parallel to the skew in bridges skewed beyond 20°. Carrying cross-frames and diaphragms parallel to the skew angle in bridges skewed more than 20° is a practice implemented by some state DOTs, and is primarily done to minimize problems with cross-frame fit-up during erection.

The authors have performed a study to investigate the effects of cross-frame orientation and skew angle upon lateral flange bending stresses, by examining lateral flange bending stresses in a suite of detailed 3D, solid finite element analyses of skewed bridge systems, in which cross-frame layout, spacing, and skew angle were varied. Skewed bridge systems with cross-frames placed parallel to the skew angle as well as systems with cross-frames arranged in a staggered configuration were considered. The models included both material and geometric nonlinearities to assess the lateral flange bending stresses in the different bridge systems.

The findings of this study showed that cross-frames placed parallel to the angle of skew produced significantly lower values for f_l than cases in which cross-frames were placed perpendicular to the girder line and staggered. Both reducing the skew angle and decreasing cross-frame spacing were found to reduce lateral flange bending stresses. The values of lateral flange bending stress for all configurations were greater than the bounds of the approximate

values suggested by AASHTO. Moreover, the minimum values for f_l provided in the AASHTO-LRFD Bridge Design Specifications were found to be significantly lower than the results obtained from this study.

Acknowledgements

The authors of this report would like to gratefully acknowledge the Kansas DOT, for their support of the work performed under this project, and for knowledgeable guidance and input provided by Mr. John Jones throughout the project activities.

Table of Contents

List of Tables

List of Figures

1. Introduction and Background

The American Association of State Highway and Transportation Officials (AASHTO) provisions for lateral flange bending stresses are based on the assumption that cross-frames are oriented perpendicular to the girder line whenever the skew angle is greater than 20 degrees. Current Kansas Department of Transportation (KDOT) design practice is to align cross-frames parallel to the skew angle to avoid problems associated with fit-up and distortion-induced fatigue. There is a potentially significant discrepancy between assumptions implicit in the AASHTO Specifications and bridges that are designed to be skewed between 20 and 40 degrees that include cross-frames placed parallel to the skew.

The objectives of this study were to quantify the effects of cross-frame orientation and cross-frame spacing on lateral flange bending stresses during the bridge construction phase and to evaluate AASHTO's interaction requirement of weak-axis bending demands with strong-axis demands on the flanges. Stability is especially of concern during construction stages, before a composite concrete deck has hardened; in this stage, steel girders rely on intermediate cross-frames for stability. Detailed three-dimensional solid finite element models were used to investigate these parameters (skew angle, cross-frame spacing, and cross-frame orientation).

2. Bridge Geometry

The bridge geometry used within this study was adapted from American Iron and Steel Institute (AISI) Design Example 2 (AISI, 1997). This geometry can be considered typical of a multi-girder highway overpass and its design is well understood and widely available. The bridge has two 27.4 m [90 ft] spans, composed of four continuous girders spaced at 3.1 m [10 ft] as presented in Fig. 1. Girders were non-composite, topped by a 203 mm [8.0 in] thick wet concrete deck with a 1.1 m [3.5 ft] roadway overhang and a 0.7 m [2.3 ft] construction walkway. The total deck width was 12.7 m [41.7 ft]. Both the roadway overhang and construction walkway were supported by 1.8 m [70 in] C-49-D overhang brackets spaced 1.0 m [40 in] on center. Separate built-up cross-sections were used in regions of positive and negative bending, as shown

in Fig. 1(a) and 1(b). Each girder was supported by a pin at the central pier and roller supports at both ends.

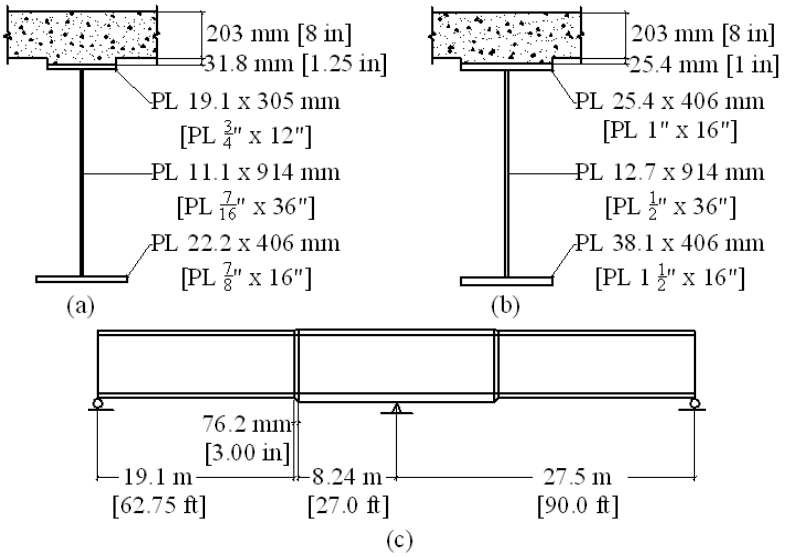

Figure 1 (a) Positive girder cross-section. (b) Negative girder cross-section. (c) Location of positive and negative cross-sections.

Bridges with skewed supports are designed as such to accommodate highway alignment. Three primary bracing configurations are used in skewed steel bridges. Bracing may be placed parallel to the skew angle, or perpendicular to the girder line in a staggered or unstaggered configuration. These configurations, shown in Fig. 2, will be referred to as skewed-parallel, skewed-staggered, and skewed-unstaggered, respectively. AASHTO requires that bracing be placed perpendicular to the girder line whenever the skew angle is greater than 20 degrees. However, KDOT design provisions allow the use of skewed-parallel configuration for angles up to 40 deg. to reduce potential differential deflection and associated distortion-induced fatigue (KDOT 2010). For the analyses performed in this study, results for the skewed-parallel and skewed-staggered configurations with 20 degree and 40 degree skews were considered. Both 4.6 m [15 ft] and 9.1 m [30 ft] cross-frame spacings were studied.

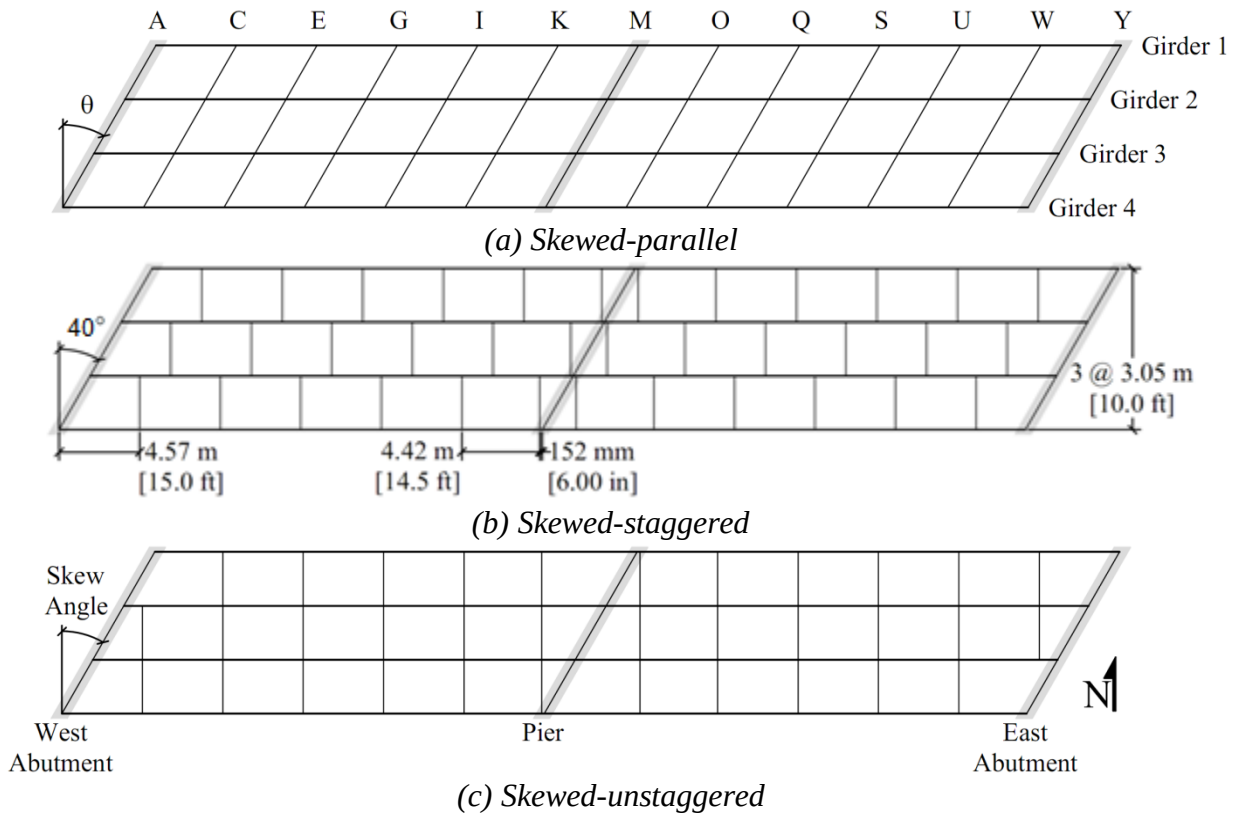

Figure 2 Bridge configurations (40 deg. skew with 4.57 m [15.0 ft] cross-frame spacing)

Cross-frames, referring to truss-type lateral braces placed at discrete locations along a bridge layout, were used in all bridge configurations studied and consisted of three equal-leg angle cross-sections spanning between connection stiffeners. A square plate was used to connect the diagonal legs, as shown in Fig. 3. In bridges with skewed-parallel configurations, cross-frame length increased with skew angle and bent plate stiffeners were used to capture realistic construction considerations. The slenderness ratio for the single angles was computed using provisions in American Institute of Steel Construction's Steel Construction Manual (AISC Manual, 2010) Section E5, and cross-frame stiffness was compared based on the approximate relative stiffness, $A\cos^3\theta$,where A is the cross-sectional area of one angle and θ is the skew angle (Yura, 2001); (Wang & Helwig, 2008). This was done to ensure that cross-frames were selected in the different models such that they had similar stiffnesses. A L108x108x12.7 mm [L4.25x4.25x0.5 in] angle was selected for the skewed-staggered bridge and a L140x140x15.9 mm [5.5x5.5x0.625 in] angle was selected for the skewed-parallel bridge. Connection stiffener

dimensions are shown in Fig. 3; a thickness of 9.53 mm [0.375 in] was selected for the skewed bridge connection stiffeners.

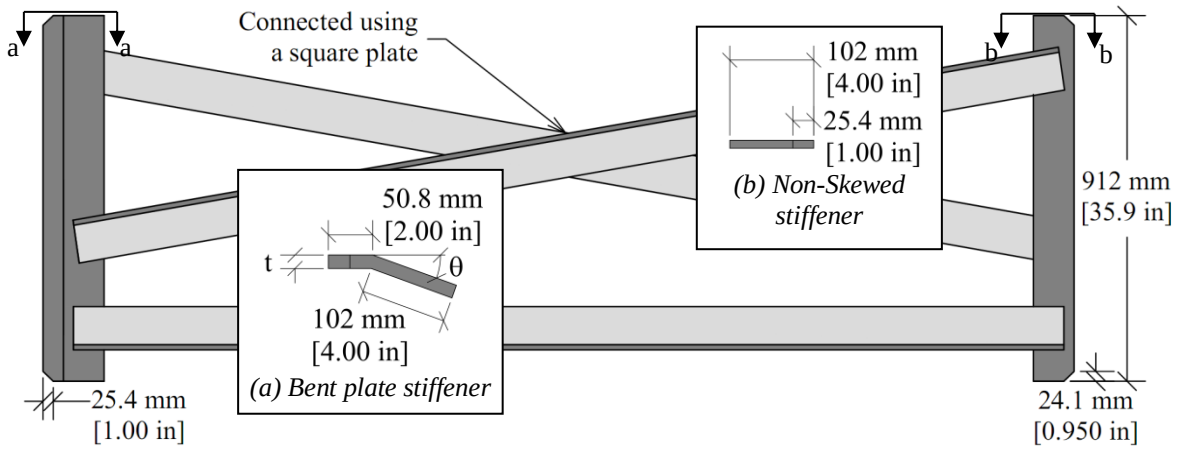

Figure 3 Connection stiffener geometry

3. MODELING METHODOLOGY

Three-dimensional, solid-element finite element (FE) models of the entire bridge were constructed using Abaqus v.6.10-2 for parametric analysis (Simulia, 2010), represented in Fig. 4. C3D8R brick elements were used for the majority of the model, but C3D4 tetrahedral and C3D6 wedge elements were used to transition between mesh sizes where needed. Both geometric nonlinearity and material nonlinearity were considered within the analyses.

Figure 4 3D FEM model geometry of skewed-staggered bridge configuration

Each of the four bridge girders were composed of the bottom flange, web, and top flange. Girder flanges and webs were composed of steel with a modulus of elasticity of 200,000 MPa [29,000 ksi] and Poisson's ratio of 0.3. The steel was defined to undergo material nonlinearity through isotropic hardening. The material plasticity data defined within Abqaus are presented in Table 1 as true stress and logarithmic plastic strain; the piecewise-linear stress-strain curve is presented in Fig. 5. A maximum mesh size of 51 mm [2 in] was used for all steel parts.

Table 1 Steel stress-strain diagram

True Stress (MPa) [ksi]	Logarithmic Plastic Strain
376.9 [54.7]	0
381.5 [55.3]	0.037
401.2 [58.2]	0.044
445.9 [64.7]	0.097
451.9 [65.5]	0.110
462.0 [67.0]	0.178

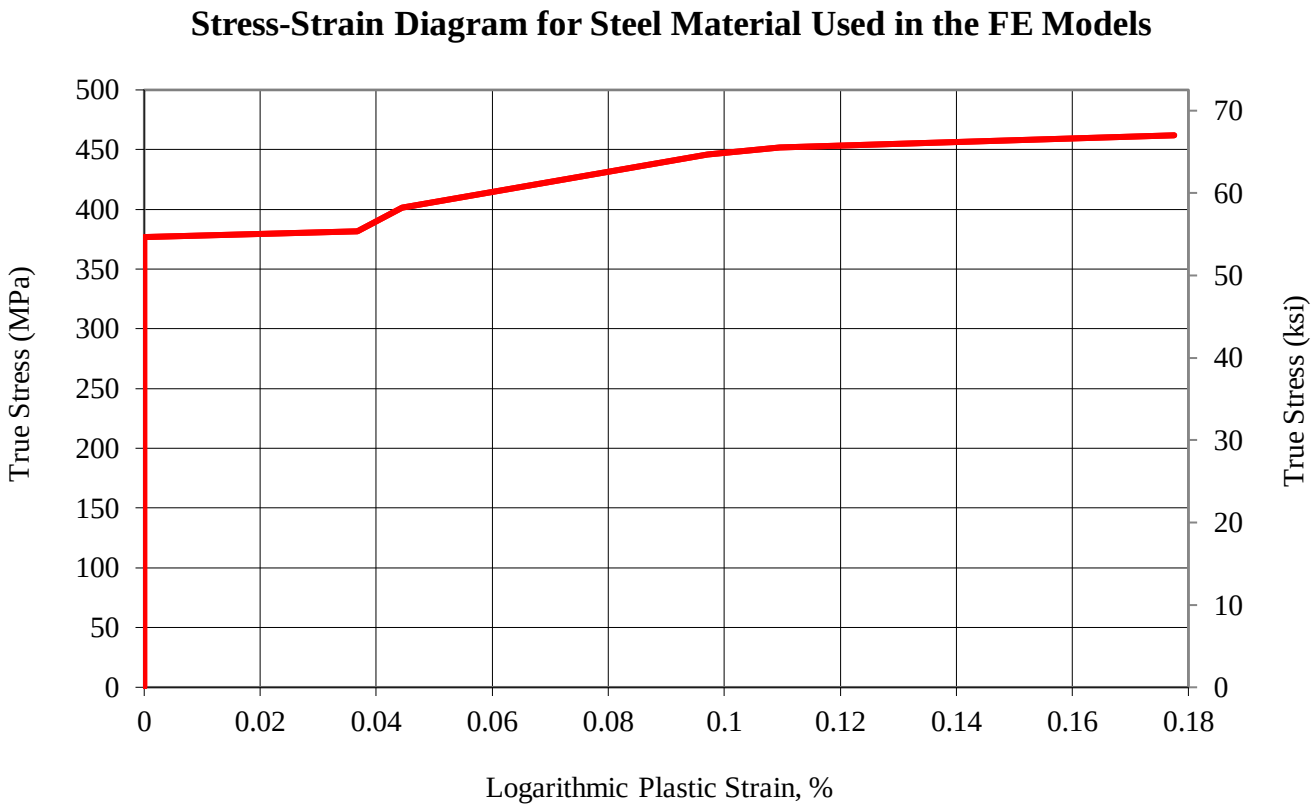

Figure 5 Steel stress-strain diagram

The steel overhang brackets were modeled with the same properties as the girders. Five 51x51 mm [2x2 in] wall stud joists (timber) supporting the construction walkway and a 102x102

mm [4x4 in] stud (timber) supporting the screed rail on each side of the bridge were modeled with a modulus of elasticity of 10,342 MPa [1,500 ksi] and Poisson's ratio of 0.2. Plywood formwork supporting the wet concrete deck, typically used during construction, was not included in the models because the stiffness contribution from the attached plywood was found to affect lateral bending stresses significantly within the models, and since real connections between plywood formwork and steel girders are not capable of developing sufficient lateral support, designers rightfully neglect the contributions of such formwork.

Given the nonlinear characteristics of the models, it was not surprising that challenges with convergence were initially encountered and high-order buckling modes occurred as a modeling artifact. To eliminate the high-order buckling mode that tended to occur in girder flanges in trial model executions, a very thin and flexible top flange cover, with the same width as the top flange, was used to damp the response in the top flange. This "soft layer" was assigned a thickness of 25 mm [1 in] in the positive moment region and 13 mm [0.5 in] in the negative moment region to accommodate the difference in thickness of the top flange in these two regions. The flange cover had a modulus of elasticity of 2760 MPa [400 ksi]. Due to its low stiffness, use of this model control technique did not affect the bending moment results, and this was verified through a comparison of models that included / did not include the compliant layer on the flange.

Surface-to-surface ties were used to attach parts. Welds were explicitly modeled to connect the flanges, webs, and cross-frame stiffeners. A mesh size of 4 mm [0.1 in] was used for welds to maintain a reasonable element aspect ratio. Welds were modeled with the same material properties as other steel parts. Interactions between the connection stiffeners and girder flanges were defined using a hard contact definition. This allowed for the connection stiffener to bear against the girder flanges when flange rotations were significant. Girder boundary conditions were modeled by applying a translational constraint over a narrow, 51 mm [2 in] strip of the bottom flange at the mid-span and ends of the girders. A pinned support was used to represent the center pier while roller supports represented abutment piers.

4. APPLIED LOADS

The following dead and live loads applied in the models during the construction stage were based on The Kansas Department of Transportation Design Manual: Volume III Section 5.3 (KDOT, 2010). Wind pressures on the structure were based on AASHTO Section 3.8 (AASHTO, 2010).

- The 203 mm [8 in] thick wet concrete deck with a density of 2563 kg/m^3 [160 lb/ft^3] was applied as a uniform pressure over the vertical projection of the web on the top flange cover and roadway overhang. The density included the weight of reinforcing steel and forms.
- A 27.2 mm [1.07 in] effective height of the concrete deck haunches was applied as a uniform pressure using a 2563 kg/m^3 [160 lb/ft^3] density over the vertical projection of the web on the top flange cover. This density included the weight of reinforcing steel and forms.
- Steel weight was applied as a gravity load using a density of 7849 kg/m^3 [490 lb/ft^3].
- A 366 kg/m^2 [75.0 lb/ft^2] construction live load was applied as a uniform pressure over the vertical projection of the web on the top flange cover.
- A 744 kg/m [500 lb/ft] screed load was applied as a uniform pressure over a width of 102 mm [4.00 in] on the plywood screed rail.
- A 801 kg/m^3 [50.0 lb/ft^3] walkway load was applied as a uniform pressure over the construction walkway surface.
- A 244 kg/m^2 [50.0 lb/ft^2] traverse wind load was applied over the lateral surface area of the deck exterior on either the south side in Fig. 2 (right side in Fig. 4) or north side in Fig. 2 (left side in Fig. 4). A longitudinal wind pressure was not considered.
- A vertical upward wind force of 97.6 kg/m^2 [20 lb/ft^2] times the width of the deck, including parapets and sidewalks, was applied as a uniform pressure over the vertical projection of the webs on the top flange cover. The tributary

area was calculated as if the uplift force was a longitudinal line load at the windward quarter-point of the deck width.

- Dead and live loads from the tributary area on the deck were applied as a 13 mm [0.5 in] wide uniform pressure over the vertical projection of the web on the top flange cover. These loads were applied over the vertical web projection on the top flange cover rather than over the entire flange cover to further prevent from occurring the model artifact of high-order buckling in the top flange.

5. STRESS CALCULATIONS

A free body cross-section in Abaqus is an area of the model across which resultant forces and moments are computed. Once the cross-section is defined, Abaqus can be used to output vectors that include the magnitude and direction of the resultant moments across the area that is selected. Major axis bending moments about the girder cross-section were obtained using section cuts along Girder 3 (Fig. 2). Girder 3 was chosen because the interior girders experienced higher moments than exterior girders. The girder cross-section, which consists of the top flange, web, and bottom flange, is shown in Fig. 6(a) along with the resultant moments.

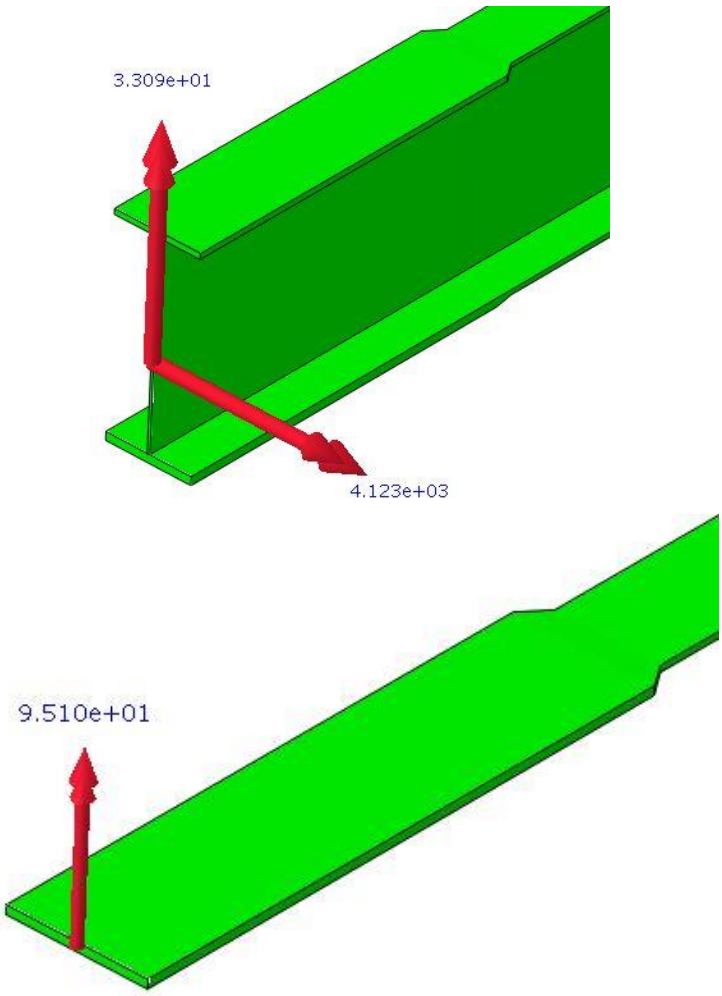

(a) Girder Section *(b) Top Flange Section*

Figure 6 Resultant moments displayed on the free body section

Lateral flange bending moments were computed from both the top and bottom flanges individually using a procedure described in Jung & White (2006) as well as from the entire girder section. The top flange section cut is shown in Fig. 6(b) along with the resultant lateral flange bending moment. Moment values were measured at locations where the cross-frames connected to the web (where lateral flange bending stresses were expected to be at a maximum) and at the mid-point between two cross-frame locations along the girder (where localized effects were expected to be least influential). Flexural stresses, σ, were calculated from these moments using the bending stress equation:

$\sigma = Mc/I$

where

M = flange or section bending moment

c = distance from the extreme fiber to the neutral axis

I = moment of inertia of the flange or section

The top flange had a *c* value of 152 mm [6 in] and an *I* value of 4.50×10^{-5} m^4 [108 in^4] in the positive flexure region and a *c* value of 203 mm [8 in] and an *I* value of 1.42×10^{-4} m^4 [341 in^4] in the negative flexure region. The bottom flange had a *c* value of 203 mm [8 in] and an *I* value of 1.24×10^{-4} m^4 [108 in^4] in the positive flexure region and a *c* value of 203 mm [8 in] and an *I* value of 2.13×10^{-4} m^4 [341 in^4] in the negative flexure region. The *c* value for the girder section was taken as 203 mm [8 in] in weak axis bending for both the positive and negative flexure regions.

AASHTO (2010) presents interaction requirements combining minor-axis bending demands with major-axis demands based on factored loads:

$f_{bu} + \frac{1}{3} f_l \leq \phi_f F_{nc}$ (AASHTO 6.10.8.1.1-1)

where

f_{bu} = major-axis demand (ksi)

f_l = minor-axis demand (ksi)

ϕ_f = resistance factor for flexure, 1.0

F_{nc} = nominal resistance factor, 50 ksi

In lieu of refined analysis, AASHTO permits engineers to use a minimum of f_l = 69 MPa [10 ksi] for interior girders and f_l = 52 MPa [7.5 ksi] for exterior girders. These values are based on a limited data set for skewed bridges. Therefore, it is important to further examine lateral flange bending stresses through refined analysis.

Load combinations and load factors are presented in AASHTO Section 3.4 (AASHTO, 2010). The Strength load combinations and load factors from AASHTO Table 3.4.1-1 were found to produce the controlling load combination during the construction stage:

Strength 1 (S1): 1.25 DC + 1.25 DW + 1.75 LL

Strength 3 (S2): 1.25 DC + 1.25 DW + 1.4 WS (including uplift)

Strength 4 (S4): 1.50 DC + 1.50 DW

Strength 5 (S5): 1.25 DC + 1.25 DW + 1.35 LL + 0.4 WS (no uplift)

where

DC = dead load of structural components

DW = dead load of wearing surface

LL = construction live load

WS = wind load on structure

6. RESULTS

Table 2 through 6 show the peak major axis bending stress, peak lateral flange bending stress, the AASHTO interaction equation result, and a calculated safety factor for five different bridge configurations. Safety factors were calculated based on a steel yield strength of 345 MPa [50 ksi]. Maximum lateral flange bending stresses calculated from the top flange, bottom flange, and overall girder section are presented. Results from both the positive flexure region and negative flexure region of the bridge are shown.

From the results, Strength 1 produced the highest interaction equation results and lowest safety factors for all bridge configurations. The negative flexure region produced lower safety factors than the positive flexure region of the bridge. The highest lateral flange bending stresses were calculated based on moments obtained from the top flange in the positive moment region, while lateral flange bending stresses calculated from the bottom flange and girder section were generally much lower in that region. The negative flexure region produced much lower lateral

flange bending stresses. The skewed-staggered and skewed-parallel configurations produced relatively similar interaction equation results. However, skewed-parallel configurations typically produced lower lateral flange bending stresses than skewed-staggered configurations.

The 40 degree skewed-staggered with 9.1 m [30 ft] cross-frame spacing bridge configuration produced significantly higher lateral flange bending stresses in the top flange for the Strength 1 load combination than the 40 degree skewed-staggered with 4.6 m [15 ft] cross-frame spacing bridge configuration. The highest lateral flange bending stress was found to be 243 MPa [35 ksi] in the top flange for Strength 1 in the 40 degree skewed-staggered with 9.14 m [30 ft] cross-frame spacing bridge configuration.

AASHTO's interaction equation results were generally similar between 40 degree and 20 degree skewed configurations. However, Strength 1 lateral flange bending stress calculated from the top flange were significantly higher in the 40 degree skewed bridges. The 40 degree skewed-staggered bridge configuration produced a peak lateral flange bending stress of 176 MPa [25.5 ksi] compared to 126 MPa [18.3 ksi] for the 20 degree skewed-staggered bridge configuration. Similarly, the 40 degree skewed-parallel bridge configuration produced a peak lateral flange bending stress of 155 MPa [22.5 ksi] compared to 155 MPa [13.3 ksi] for the 20 degree skewed-staggered bridge configuration.

The deformed shape of the 40 deg. skewed-parallel with 4.57 m [15.0 ft] cross-frame spacing bridge configuration is shown in Fig. 7 for reference. Unfactored loads were applied, and wind loads were not considered since the controlling load combination was found to be Strength 1. The scale factor for displacement was set to one. The stress contours shown in Fig. 7 are Von Mises stresses, with the color map limits set between 0 and 345 MPa [50 ksi]. High stress regions occurred in the flanges over the interior support.

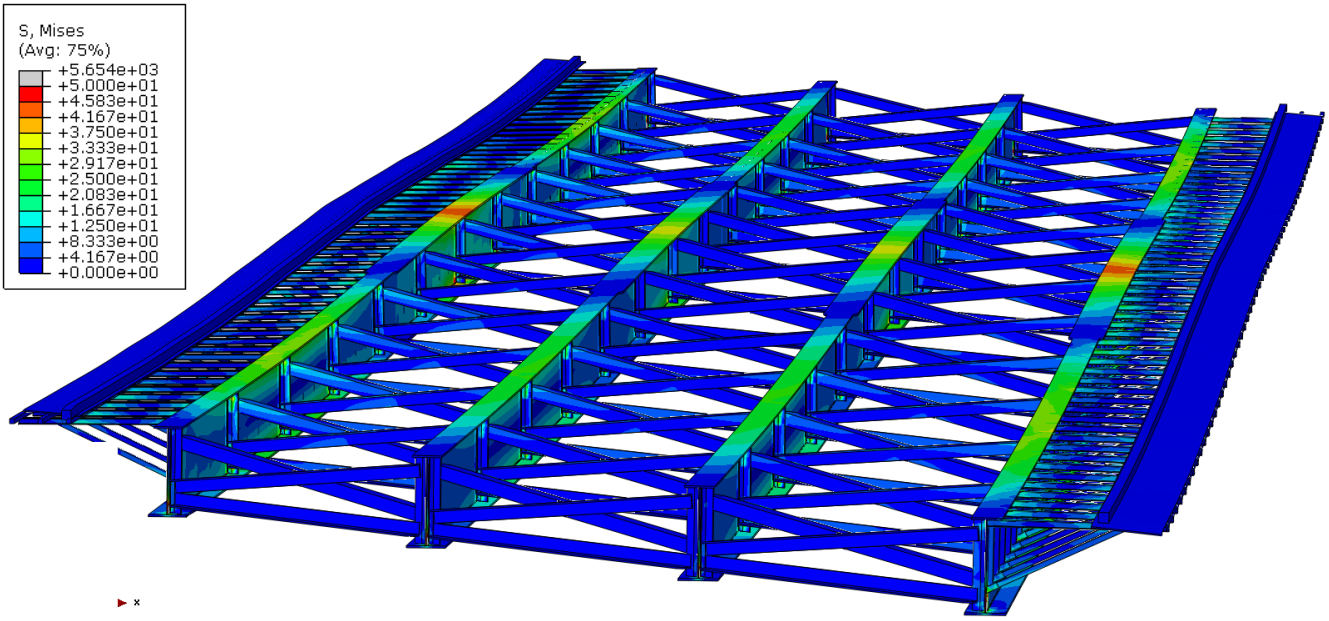

Figure 7 Deformed shape of the 40 deg. skewed-parallel with 4.57 m [15.0 ft] cross-frame spacing

Table 2 AASHTO's interaction equation results for 40 degree skewed-staggered with 4.6 m [15 ft] cross-frame spacing

Load Combination	f_{bu} (MPa) [ksi]	f_l (MPa) [ksi]	$[f_{bu} + 1/3\, f_l]$ (MPa) [ksi]	Safety Factor
Strength 1	195 [28.3]	176 [25.5]	254 [36.8]	1.36
Strength 3 (wind North)	90 [13.1]	55 [8.0]	109 [15.8]	3.17
Strength 3 (wind South)	67 [9.7]	35 [5.0]	78 [11.3]	4.41
Strength 4	123 [17.8]	39 [5.6]	136 [19.7]	2.54
Strength 5 (wind North)	171 [24.9]	103 [15.0]	206 [29.9]	1.67
Strength 5 (wind South)	171 [24.9]	99 [14.3]	204 [29.7]	1.69

a) Top Flange – Positive Flexure Region

Load Combination	f_{bu} (MPa) [ksi]	f_l (MPa) [ksi]	$[f_{bu} + 1/3\, f_l]$ (MPa) [ksi]	Safety Factor
Strength 1	225 [32.7]	93 [13.4]	256 [37.1]	1.35
Strength 3 (wind North)	107 [15.5]	22 [3.1]	114 [16.5]	3.03
Strength 3 (wind South)	78 [11.4]	26 [3.7]	87 [12.6]	3.96
Strength 4	145 [21.0]	11 [1.6]	148 [21.5]	2.32
Strength 5 (wind North)	196 [28.4]	52 [7.5]	213 [30.9]	1.62
Strength 5 (wind South)	195 [28.3]	45 [6.6]	210 [30.5]	1.64

a) Top Flange – Negative Flexure Region

Load Combination	f_{bu} (MPa) [ksi]	f_l (MPa) [ksi]	$[f_{bu} + 1/3\, f_l]$ (MPa) [ksi]	Safety Factor
Strength 1	195 [28.3]	80 [11.6]	222 [32.2]	1.55
Strength 3 (wind North)	90 [13.1]	29 [4.2]	100 [14.5]	3.45
Strength 3 (wind South)	67 [9.7]	27 [3.9]	76 [11.0]	4.56
Strength 4	123 [17.8]	23 [3.3]	130 [18.9]	2.64
Strength 5 (wind North)	171 [24.9]	41 [5.9]	185 [26.8]	1.86
Strength 5 (wind South)	171 [24.9]	44 [6.4]	186 [27.0]	1.85

b) Bottom Flange – Positive Flexure Region

Load Combination	f_{bu} (MPa) [ksi]	f_l (MPa) [ksi]	$[f_{bu} + 1/3\, f_l]$ (MPa) [ksi]	Safety Factor
Strength 1	225 [32.7]	77 [11.2]	251 [36.4]	1.37
Strength 3 (wind North)	107 [15.5]	9 [1.3]	110 [15.9]	3.14
Strength 3 (wind South)	78 [11.4]	15 [2.2]	83 [12.1]	4.13
Strength 4	145 [21.0]	10 [1.4]	148 [21.5]	2.33
Strength 5 (wind North)	196 [28.4]	48 [7.0]	212 [30.7]	1.63
Strength 5 (wind South)	195 [28.3]	47 [6.8]	211 [30.6]	1.63

b) Bottom Flange – Negative Flexure Region

Load Combination	f_{bu} (MPa) [ksi]	f_l (MPa) [ksi]	$[f_{bu} + 1/3\, f_l]$ (MPa) [ksi]	Safety Factor
Strength 1	195 [28.3]	37 [5.3]	207 [30.1]	1.66
Strength 3 (wind North)	90 [13.1]	12 [1.7]	94 [13.7]	3.66
Strength 3 (wind South)	67 [9.7]	23 [3.3]	74 [10.8]	4.65
Strength 4	123 [17.8]	8 [1.2]	125 [18.2]	2.75
Strength 5 (wind North)	171 [24.9]	25 [3.6]	180 [26.0]	1.92
Strength 5 (wind South)	171 [24.9]	21 [3.0]	178 [25.9]	1.93

c) Girder Section – Positive Flexure Region

Load Combination	f_{bu} (MPa) [ksi]	f_l (MPa) [ksi]	$[f_{bu} + 1/3\, f_l]$ (MPa) [ksi]	Safety Factor
Strength 1	225 [32.7]	18 [2.6]	231 [33.5]	1.49
Strength 3 (wind North)	107 [15.5]	6 [0.9]	109 [15.8]	3.17
Strength 3 (wind South)	78 [11.4]	17 [2.5]	84 [12.2]	4.10
Strength 4	145 [21.0]	3 [0.4]	146 [21.2]	2.36
Strength 5 (wind North)	196 [28.4]	12 [1.8]	200 [29.0]	1.73
Strength 5 (wind South)	195 [28.3]	11 [1.7]	199 [28.9]	1.73

c) Girder Section – Negative Flexure Region

Table 3 AASHTO interaction equation results for 40 degree skewed-parallel with 4.6 m [15 ft] cross-frame spacing

Load Combination	f_{bu} (MPa) [ksi]	f_l (MPa) [ksi]	$[f_{bu} + 1/3 f_l]$ (MPa) [ksi]	Safety Factor
Strength 1	191 [27.7]	155 [22.5]	243 [35.2]	1.42
Strength 3 (wind North)	94 [13.6]	7 [1.1]	96 [14.0]	3.57
Strength 3 (wind South)	72 [10.5]	15 [2.2]	77 [11.2]	4.46
Strength 4	129 [18.8]	6 [0.8]	131 [19.0]	2.63
Strength 5 (wind North)	180 [26.1]	85 [12.4]	208 [30.2]	1.66
Strength 5 (wind South)	180 [26.2]	77 [11.2]	206 [29.9]	1.67

a) Top Flange – Positive Flexure Region

Load Combination	f_{bu} (MPa) [ksi]	f_l (MPa) [ksi]	$[f_{bu} + 1/3 f_l]$ (MPa) [ksi]	Safety Factor
Strength 1	224 [32.5]	17 [2.4]	230 [33.3]	1.50
Strength 3 (wind North)	111 [16.2]	11 [1.6]	115 [16.7]	3.00
Strength 3 (wind South)	83 [12.1]	29 [4.2]	93 [13.5]	3.71
Strength 4	151 [21.9]	8 [1.2]	154 [22.3]	2.24
Strength 5 (wind North)	206 [29.8]	19 [2.8]	212 [30.7]	1.63
Strength 5 (wind South)	205 [29.7]	14 [2.0]	210 [30.4]	1.65

a) Top Flange – Negative Flexure Region

Load Combination	f_{bu} (MPa) [ksi]	f_l (MPa) [ksi]	$[f_{bu} + 1/3 f_l]$ (MPa) [ksi]	Safety Factor
Strength 1	191 [27.7]	24 [3.5]	199 [28.9]	1.73
Strength 3 (wind North)	94 [13.6]	11 [1.5]	98 [14.2]	3.53
Strength 3 (wind South)	72 [10.5]	34 [5.0]	84 [12.1]	4.12
Strength 4	129 [18.8]	3 [0.4]	130 [18.9]	2.65
Strength 5 (wind North)	180 [26.1]	20 [2.9]	186 [27.0]	1.85
Strength 5 (wind South)	180 [26.2]	21 [3.0]	187 [27.2]	1.84

b) Bottom Flange – Positive Flexure Region

Load Combination	f_{bu} (MPa) [ksi]	f_l (MPa) [ksi]	$[f_{bu} + 1/3 f_l]$ (MPa) [ksi]	Safety Factor
Strength 1	224 [32.5]	19 [2.8]	230 [33.4]	1.50
Strength 3 (wind North)	111 [16.2]	13 [1.9]	116 [16.8]	2.98
Strength 3 (wind South)	83 [12.1]	27 [3.9]	92 [13.4]	3.74
Strength 4	151 [21.9]	11 [1.6]	155 [22.5]	2.23
Strength 5 (wind North)	206 [29.8]	18 [2.6]	212 [30.7]	1.63
Strength 5 (wind South)	205 [29.7]	22 [3.2]	212 [30.8]	1.62

b) Bottom Flange – Negative Flexure Region

Load Combination	f_{bu} (MPa) [ksi]	f_l (MPa) [ksi]	$[f_{bu} + 1/3 f_l]$ (MPa) [ksi]	Safety Factor
Strength 1	191 [27.7]	73 [10.6]	215 [31.2]	1.60
Strength 3 (wind North)	94 [13.6]	8 [1.2]	97 [14.0]	3.56
Strength 3 (wind South)	72 [10.5]	25 [3.7]	81 [11.7]	4.27
Strength 4	129 [18.8]	2 [0.3]	130 [18.9]	2.65
Strength 5 (wind North)	180 [26.1]	44 [6.4]	195 [28.2]	1.77
Strength 5 (wind South)	180 [26.2]	42 [6.1]	194 [28.2]	1.77

c) Girder Section – Positive Flexure Region

Load Combination	f_{bu} (MPa) [ksi]	f_l (MPa) [ksi]	$[f_{bu} + 1/3 f_l]$ (MPa) [ksi]	Safety Factor
Strength 1	224 [32.5]	11 [1.7]	228 [33.0]	1.51
Strength 3 (wind North)	111 [16.2]	11 [1.6]	115 [16.7]	2.99
Strength 3 (wind South)	83 [12.1]	25 [3.6]	92 [13.3]	3.77
Strength 4	151 [21.9]	6 [0.9]	153 [22.2]	2.25
Strength 5 (wind North)	206 [29.8]	11 [1.6]	209 [30.3]	1.65
Strength 5 (wind South)	205 [29.7]	11 [1.7]	209 [30.3]	1.65

c) Girder Section – Negative Flexure Region

Table 4 AASHTO interaction equation results for 40 degree skewed-staggered with 9.1 m [30 ft] cross-frame spacing

Load Combination	f_{bu} (MPa) [ksi]	f_l (MPa) [ksi]	$[f_{bu} + 1/3 f_l]$ (MPa) [ksi]	Safety Factor
Strength 1	168 [24.3]	243 [35.3]	249 [36.1]	1.39
Strength 3 (wind North)	100 [14.4]	68 [9.8]	122 [17.7]	2.82
Strength 3 (wind South)	58 [8.4]	52 [7.6]	75 [10.9]	4.60
Strength 4	126 [18.2]	22 [3.2]	133 [19.3]	2.59
Strength 5 (wind North)	158 [22.9]	115 [16.7]	197 [28.5]	1.75
Strength 5 (wind South)	158 [23.0]	100 [14.5]	191 [27.8]	1.80

a) Top Flange – Positive Flexure Region

Load Combination	f_{bu} (MPa) [ksi]	f_l (MPa) [ksi]	$[f_{bu} + 1/3 f_l]$ (MPa) [ksi]	Safety Factor
Strength 1	207 [30.1]	80 [11.5]	234 [33.9]	1.48
Strength 3 (wind North)	116 [16.9]	40 [5.8]	130 [18.8]	2.66
Strength 3 (wind South)	68 [9.9]	31 [4.5]	78 [11.4]	4.39
Strength 4	147 [21.3]	3 [0.5]	148 [21.4]	2.33
Strength 5 (wind North)	184 [26.6]	33 [4.8]	195 [28.2]	1.77
Strength 5 (wind South)	183 [26.5]	26 [3.7]	191 [27.8]	1.80

a) Top Flange – Negative Flexure Region

Load Combination	f_{bu} (MPa) [ksi]	f_l (MPa) [ksi]	$[f_{bu} + 1/3 f_l]$ (MPa) [ksi]	Safety Factor
Strength 1	168 [24.3]	110 [16.0]	205 [29.7]	1.69
Strength 3 (wind North)	100 [14.4]	32 [4.7]	110 [16.0]	3.13
Strength 3 (wind South)	58 [8.4]	45 [6.5]	73 [10.5]	4.75
Strength 4	126 [18.2]	24 [3.5]	134 [19.4]	2.58
Strength 5 (wind North)	158 [22.9]	45 [6.5]	173 [25.1]	1.99
Strength 5 (wind South)	158 [23.0]	54 [7.9]	176 [25.6]	1.95

b) Bottom Flange – Positive Flexure Region

Load Combination	f_{bu} (MPa) [ksi]	f_l (MPa) [ksi]	$[f_{bu} + 1/3 f_l]$ (MPa) [ksi]	Safety Factor
Strength 1	207 [30.1]	47 [6.9]	223 [32.3]	1.55
Strength 3 (wind North)	116 [16.9]	19 [2.7]	123 [17.8]	2.81
Strength 3 (wind South)	68 [9.9]	25 [3.6]	76 [11.1]	4.52
Strength 4	147 [21.3]	7 [1.0]	149 [21.6]	2.32
Strength 5 (wind North)	184 [26.6]	22 [3.1]	191 [27.7]	1.81
Strength 5 (wind South)	183 [26.5]	25 [3.6]	191 [27.7]	1.80

b) Bottom Flange – Negative Flexure Region

Load Combination	f_{bu} (MPa) [ksi]	f_l (MPa) [ksi]	$[f_{bu} + 1/3 f_l]$ (MPa) [ksi]	Safety Factor
Strength 1	168 [24.3]	124 [17.9]	209 [30.3]	1.65
Strength 3 (wind North)	100 [14.4]	38 [5.5]	112 [16.3]	3.07
Strength 3 (wind South)	58 [8.4]	31 [4.5]	68 [9.8]	5.08
Strength 4	126 [18.2]	14 [2.0]	130 [18.9]	2.65
Strength 5 (wind North)	158 [22.9]	52 [7.5]	175 [25.4]	1.97
Strength 5 (wind South)	158 [23.0]	40 [5.8]	172 [24.9]	2.01

c) Girder Section – Positive Flexure Region

Load Combination	f_{bu} (MPa) [ksi]	f_l (MPa) [ksi]	$[f_{bu} + 1/3 f_l]$ (MPa) [ksi]	Safety Factor
Strength 1	207 [30.1]	21 [3.1]	214 [31.1]	1.61
Strength 3 (wind North)	116 [16.9]	25 [3.6]	125 [18.1]	2.77
Strength 3 (wind South)	68 [9.9]	23 [3.4]	76 [11.0]	4.55
Strength 4	147 [21.3]	4 [0.6]	148 [21.5]	2.33
Strength 5 (wind North)	184 [26.6]	10 [1.5]	187 [27.1]	1.84
Strength 5 (wind South)	183 [26.5]	8 [1.1]	185 [26.9]	1.86

c) Girder Section – Negative Flexure Region

Table 5 AASHTO interaction equation results for 20 degree skewed-staggered with 4.6 m [15 ft] cross-frame spacing

Load Combination	f_{bu} (MPa) [ksi]	f_l (MPa) [ksi]	$[f_{bu} + 1/3 f_l]$ (MPa) [ksi]	Safety Factor
Strength 1	184 [26.8]	126 [18.3]	226 [32.8]	1.52
Strength 3 (wind North)	90 [13.1]	44 [6.3]	105 [15.2]	3.29
Strength 3 (wind South)	68 [9.8]	36 [5.2]	80 [11.6]	4.33
Strength 4	123 [17.9]	24 [3.4]	131 [19.0]	2.63
Strength 5 (wind North)	174 [25.3]	100 [14.5]	207 [30.1]	1.66
Strength 5 (wind South)	177 [25.7]	96 [14.0]	209 [30.4]	1.65

a) Top Flange – Positive Flexure Region

Load Combination	f_{bu} (MPa) [ksi]	f_l (MPa) [ksi]	$[f_{bu} + 1/3 f_l]$ (MPa) [ksi]	Safety Factor
Strength 1	239 [34.6]	33 [4.8]	250 [36.2]	1.38
Strength 3 (wind North)	124 [17.9]	26 [3.8]	132 [19.2]	2.60
Strength 3 (wind South)	90 [13.1]	24 [3.5]	98 [14.3]	3.51
Strength 4	166 [24.1]	7 [1.1]	169 [24.5]	2.04
Strength 5 (wind North)	226 [32.8]	26 [3.8]	235 [34.1]	1.47
Strength 5 (wind South)	224 [32.6]	20 [3.0]	231 [33.5]	1.49

a) Top Flange – Negative Flexure Region

Load Combination	f_{bu} (MPa) [ksi]	f_l (MPa) [ksi]	$[f_{bu} + 1/3 f_l]$ (MPa) [ksi]	Safety Factor
Strength 1	184 [26.8]	51 [7.4]	201 [29.2]	1.71
Strength 3 (wind North)	90 [13.1]	30 [4.3]	100 [14.5]	3.44
Strength 3 (wind South)	68 [9.8]	26 [3.7]	76 [11.1]	4.52
Strength 4	123 [17.9]	16 [2.3]	128 [18.6]	2.69
Strength 5 (wind North)	174 [25.3]	44 [6.4]	189 [27.4]	1.82
Strength 5 (wind South)	177 [25.7]	45 [6.5]	192 [27.9]	1.79

b) Bottom Flange – Positive Flexure Region

Load Combination	f_{bu} (MPa) [ksi]	f_l (MPa) [ksi]	$[f_{bu} + 1/3 f_l]$ (MPa) [ksi]	Safety Factor
Strength 1	239 [34.6]	26 [3.7]	247 [35.9]	1.39
Strength 3 (wind North)	124 [17.9]	22 [3.2]	131 [19.0]	2.63
Strength 3 (wind South)	90 [13.1]	20 [2.9]	97 [14.1]	3.55
Strength 4	166 [24.1]	4 [0.6]	168 [24.3]	2.05
Strength 5 (wind North)	226 [32.8]	21 [3.0]	233 [33.8]	1.48
Strength 5 (wind South)	224 [32.6]	21 [3.1]	232 [33.6]	1.49

b) Bottom Flange – Negative Flexure Region

Load Combination	f_{bu} (MPa) [ksi]	f_l (MPa) [ksi]	$[f_{bu} + 1/3 f_l]$ (MPa) [ksi]	Safety Factor
Strength 1	184 [26.8]	21 [3.0]	191 [27.7]	1.80
Strength 3 (wind North)	90 [13.1]	16 [2.3]	96 [13.9]	3.60
Strength 3 (wind South)	68 [9.8]	16 [2.4]	73 [10.6]	4.72
Strength 4	123 [17.9]	6 [0.8]	125 [18.1]	2.76
Strength 5 (wind North)	174 [25.3]	18 [2.6]	180 [26.1]	1.91
Strength 5 (wind South)	177 [25.7]	15 [2.1]	182 [26.4]	1.89

c) Girder Section – Positive Flexure Region

Load Combination	f_{bu} (MPa) [ksi]	f_l (MPa) [ksi]	$[f_{bu} + 1/3 f_l]$ (MPa) [ksi]	Safety Factor
Strength 1	239 [34.6]	10 [1.4]	242 [35.1]	1.42
Strength 3 (wind North)	124 [17.9]	24 [3.4]	132 [19.1]	2.62
Strength 3 (wind South)	90 [13.1]	21 [3.1]	97 [14.1]	3.54
Strength 4	166 [24.1]	2 [0.3]	167 [24.2]	2.06
Strength 5 (wind North)	226 [32.8]	9 [1.4]	230 [33.3]	1.50
Strength 5 (wind South)	224 [32.6]	9 [1.3]	227 [33.0]	1.52

c) Girder Section – Negative Flexure Region

Table 6 AASHTO interaction equation results for 20 degree skewed-parallel with 4.6 m [15 ft] cross-frame spacing

Load Combination	f_{bu} (MPa) [ksi]	f_l (MPa) [ksi]	$[f_{bu} + 1/3 f_l]$ (MPa) [ksi]	Safety Factor
Strength 1	208 [30.2]	92 [13.3]	239 [34.6]	1.45
Strength 3 (wind North)	90 [13.0]	15 [2.2]	95 [13.8]	3.63
Strength 3 (wind South)	71 [10.3]	14 [2.1]	76 [11.0]	4.55
Strength 4	124 [18.0]	4 [0.6]	125 [18.2]	2.75
Strength 5 (wind North)	82 [11.9]	31 [4.5]	92 [13.4]	3.73
Strength 5 (wind South)	181 [26.2]	25 [3.6]	189 [27.4]	1.83

a) Top Flange – Positive Flexure Region

Load Combination	f_{bu} (MPa) [ksi]	f_l (MPa) [ksi]	$[f_{bu} + 1/3 f_l]$ (MPa) [ksi]	Safety Factor
Strength 1	264 [38.3]	13 [1.9]	269 [39.0]	1.28
Strength 3 (wind North)	123 [17.9]	30 [4.4]	133 [19.3]	2.59
Strength 3 (wind South)	94 [13.7]	30 [4.3]	104 [15.1]	3.31
Strength 4	167 [24.3]	4 [0.5]	168 [24.4]	2.05
Strength 5 (wind North)	80 [11.7]	16 [2.3]	86 [12.4]	4.03
Strength 5 (wind South)	234 [33.9]	11 [1.6]	238 [34.5]	1.45

a) Top Flange – Negative Flexure Region

Load Combination	f_{bu} (MPa) [ksi]	f_l (MPa) [ksi]	$[f_{bu} + 1/3 f_l]$ (MPa) [ksi]	Safety Factor
Strength 1	208 [30.2]	16 [2.3]	213 [30.9]	1.62
Strength 3 (wind North)	90 [13.0]	26 [3.7]	98 [14.3]	3.51
Strength 3 (wind South)	71 [10.3]	26 [3.8]	80 [11.6]	4.33
Strength 4	124 [18.0]	2 [0.2]	124 [18.0]	2.77
Strength 5 (wind North)	82 [11.9]	9 [1.3]	85 [12.3]	4.05
Strength 5 (wind South)	181 [26.2]	11 [1.7]	184 [26.7]	1.87

b) Bottom Flange – Positive Flexure Region

Load Combination	f_{bu} (MPa) [ksi]	f_l (MPa) [ksi]	$[f_{bu} + 1/3 f_l]$ (MPa) [ksi]	Safety Factor
Strength 1	264 [38.3]	15 [2.1]	269 [39.0]	1.28
Strength 3 (wind North)	123 [17.9]	28 [4.1]	132 [19.2]	2.60
Strength 3 (wind South)	94 [13.7]	28 [4.1]	104 [15.0]	3.33
Strength 4	167 [24.3]	6 [0.9]	169 [24.6]	2.04
Strength 5 (wind North)	80 [11.7]	15 [2.2]	85 [12.4]	4.03
Strength 5 (wind South)	234 [33.9]	19 [2.7]	240 [34.9]	1.43

b) Bottom Flange – Negative Flexure Region

Load Combination	f_{bu} (MPa) [ksi]	f_l (MPa) [ksi]	$[f_{bu} + 1/3 f_l]$ (MPa) [ksi]	Safety Factor
Strength 1	208 [30.2]	43 [6.3]	222 [32.3]	1.55
Strength 3 (wind North)	90 [13.0]	19 [2.7]	96 [13.9]	3.59
Strength 3 (wind South)	71 [10.3]	19 [2.8]	77 [11.2]	4.45
Strength 4	124 [18.0]	2 [0.2]	124 [18.0]	2.77
Strength 5 (wind North)	82 [11.9]	6 [0.9]	84 [12.2]	4.09
Strength 5 (wind South)	181 [26.2]	16 [2.3]	186 [26.9]	1.86

c) Girder Section – Positive Flexure Region

Load Combination	f_{bu} (MPa) [ksi]	f_l (MPa) [ksi]	$[f_{bu} + 1/3 f_l]$ (MPa) [ksi]	Safety Factor
Strength 1	264 [38.3]	9 [1.3]	267 [38.8]	1.29
Strength 3 (wind North)	123 [17.9]	27 [4.0]	132 [19.2]	2.61
Strength 3 (wind South)	94 [13.7]	27 [4.0]	103 [15.0]	3.33
Strength 4	167 [24.3]	4 [0.5]	168 [24.4]	2.05
Strength 5 (wind North)	80 [11.7]	9 [1.3]	83 [12.1]	4.13
Strength 5 (wind South)	234 [33.9]	12 [1.7]	238 [34.5]	1.45

c) Girder Section – Negative Flexure Region

7. CONCLUSIONS

The results of a study aimed at investigating the effect of skew angle and cross-frame layout on lateral flange bending stresses in skewed steel bridges showed that:

- The highest lateral flange bending stresses, produced by the Strength 1 load combination, were found to occur in the top flange of the positive flexure region of the skewed-staggered bridge.
- Maximum lateral flange bending stresses were significantly lower in bridges that utilized cross-frames placed parallel to the angle of skew than for cases in which cross-frames were placed perpendicular to the girder line and staggered.
- Reducing the skew angle decreased lateral flange bending stresses under certain load cases where these stresses were significant.
- Decreasing cross-frame spacing provided more brace support and helped reduce lateral flange bending stresses.
- The values of maximum lateral flange bending stress for the controlling load case of all configurations were greater than the values suggested by AASHTO, by as much as a factor of 3.5.

Although the results did not invalidate AASHTO's interaction equation requirements, the minimum safety factor computed was only 28 percent. Lateral flange bending stresses were found to have higher nominal values than major axis bending stresses for 40 degree skewed bridges with 4.6 m [15 ft] cross-frame spacing. Overall, lateral flange bending stresses were found to be significantly higher than the minimum values prescribed in the AASHTO-LRFD Bridge Design Specification. In the future, this study should be expanded to include other bridge geometries to further investigate this phenomenon.

8. REFERENCES

- AASHTO (2010). "LRFD Bridge Design Specifications." *American Association of State Highway and Transportation Officials,* Washington, D.C.
- AISC (2010). "Steel Construction Manual, 14th Ed." *American Institute of Steel Construction*, Chicago, IL.
- AISI Example 2: Two-Span Continuous Composite I Girder (1997). *American Iron and Steel Institute*.
- Jung, S.-K., and White, D.W. (2006). "Shear Strength of Horizontally Curved Steel I-Girders – Finite Element Analysis Studies," *Journal of Constructional Steel Research*, 62(4), 329-342.
- KDOT. (2010). "Design Manual: Volume III – Bridge Selection." *Kansas Department of Transportation*.
- Wang, L. and Helwig, T.A. (2008). "Stability Bracing Requirements for Steel Bridge Girders with Skewed Supports." *Journal of Bridge Engineering*, 13(2), 149-157.
- Yura, J. (2001). "Fundamentals of Beam Bracing." *Engineering Journal*, AISC, First Quarter, 11-26.